Available online at www.sciencedirect.com
ScienceDirect
Ceramics International 34 (2008) 2051–2057
CERAMICS INTERNATIONAL
www.elsevier.com/locate/ceramint

Microwave-induced combustion synthesis and ionic conductivity of $Ce_{0.8}(Gd_{0.2-x}Sm_x)O_{1.90}$ ceramics

Yen-Pei Fu *

Department of Materials Science and Engineering, National Dong Hwa University, Hualien 974, Taiwan

Received 18 May 2007; received in revised form 30 June 2007; accepted 31 July 2007
Available online 19 August 2007

Abstract

$Ce_{0.8}(Gd_{0.2-x}Sm_x)O_{1.90}$ nanopowders were successfully synthesized by a microwave-induced combustion process. The whole process takes only 30 min. The phase identification and morphology of resultant powders were investigated by XRD and SEM. Moreover, the correlation of ionic conductivity and thermal expansion coefficient for $Ce_{0.8}(Gd_{0.2-x}Sm_x)O_{1.90}$ ceramics from microwave-induced combustion process also is discussed in this paper. The results revealed that the bulk densities of $Ce_{0.8}(Gd_{0.2-x}Sm_x)O_{1.90}$ ceramics sintered at 1450 °C for 3 h were all greater than 95% of that in theoretical densities. The maximum electrical conductivity, $\sigma_{850°C} = 0.051$ S/cm, minimum activation energy, $E_a = 0.77$ eV and minimum thermal expansion coefficient, TEC = 18.733 ppm/°C was found at $Ce_{0.80}Gd_{0.20}O_{1.90}$ ceramic.

Keywords: C. Ionic conductivity; D. CeO_2; E. Fuel cells

1. Introduction

Solid oxide fuel cells (SOFC) are attracting widespread attention due to their high-energy conversion efficiency and low pollution. In order to reduce the operation temperature from 1000 to 800 °C or even lower, doped ceria has been considered as the solid electrolyte for moderate temperature solid oxide fuel cells [1]. At present, there is considerable interest in increasing the ionic conductivity of these materials by decreasing the grain size into the nanometer range. Grain boundaries have high defect densities and the atoms there have high mobility. These are the two important factors for increased ionic conductivity. Due to this fact, the ionic conductivity may be significantly enhanced in nanocrystalline materials compared to the microcrystalline ones [2]. Several synthesis routes have been developed to produce nanocrystalline CeO_2-based powders, such as hydrothermal synthesis [3], coprecipitation [4–6], sol–gel [7], and Pechini process [8]. CeO_2-based powders have been synthesized successfully by the combustion synthesis using different complexing agents/fuel such as glycine [9,10], and carbohydrazide [11]. With the combustion synthesis a desired homogeneous high-purity powder can be produced in a short time and low cost. In this study, I also attempted a new method, microwave-induced combustion synthesis to produce $Ce_{0.8}(Gd_{0.2-x}Sm_x)O_{1.90}$ powders. The advantages of combustion method are (1) simple process: all the reactions take only a few minutes, not like the other methods that require tedious process, (2) simple equipment: this method does not require complicated equipment, and (3) cheap sources: chemicals used in this method are cheap, unlike special materials needed in sol–gel process. Microwave processing of materials is fundamentally different from the conventional processing due to its heating mechanism. In a microwave oven, heat is generated within the sample itself by the interaction of microwaves with the material. In conventional heating, the heat is generated by heating elements, which is then transferred to the sample surfaces [12].

Microwave-induced combustion synthesis involves the dissolution of metal nitrates and urea in water, and then heating the solution in a microwave oven. The urea and metal nitrate decompose and give off flammable gases. After the solution reaches the point of spontaneous combustion, it begins burning and becomes a solid, which burns at a high temperature. Combustion is not complete until all the flammable substances are consumed, and the resulting material is a loose, highly friable substance exhibiting voids and pores

* Tel.: +886 3 863 4209; fax: +886 3 863 4200.
E-mail address: d887503@alumni.nthu.edu.tw.

0272-8842/$34.00
doi:10.1016/j.ceramint.2007.07.026

formed by the escaping gases during the combustion reaction [13]. The whole process takes only 30 min to yield nano-structured $Ce_{0.8}(Gd_{0.2-x}Sm_x)O_{1.90}$ powders. In this article, I report a detail conductivity, thermal expansion, and activation energy in the $Ce_{0.8}(Gd_{0.2-x}Sm_x)O_{1.90}$ ($0.0 \leq x \leq 0.2$) system. Thermal expansion is an important property, because it governs the performance of various high temperature devices [14]. Moreover, we investigate the relationship between the average thermal expansion coefficient and ionic conductivity of $Ce_{0.8}(Gd_{0.2-x}Sm_x)O_{1.90}$ ceramics.

2. Experimental procedures

2.1. Sample synthesis

The synthesis process involved the combustion of a redox mixture, in which metal nitrate acted as an oxidizing reactant and urea as a reducing one. Stoichiometric amounts of cerium nitrate hexahydrate ($Ce(NO_3)_3{\cdot}6H_2O$), gadolinium nitrate hexahydrate ($Gd(NO_3)_3{\cdot}6H_2O$), samarium nitrate hexahydrate ($Sm(NO_3)_3{\cdot}6H_2O$), and urea ($CO(NH_2)_2$) were dissolved in water. $Ce_{0.8}(Gd,Sm)_{0.2}(NO_3)_3$ nitrate solution with molar concentration of 1.5 M was made from cerium nitrate hexahydrate, gadolinium nitrate hexahydrate, and samarium nitrate hexahydrate. The amount of urea, which corresponds to ratio of fuel to nitrate in which the fuel can react completely with nitrate, was calculated by the concepts in propellant chemistry [15]. The stoichiometry of the redox mixture used for combustion was determined using the total oxidizing and reducing valences of the components, which served as numerical coefficients for the stoichiometric balance so that the equivalence ratio (Φ_e) was unity and the energy released by combustion was maximum. According to this concept, the valences of some elements and ions are as follows: C = +4, H = +1, O = −2, divalent metal ions = −2, and trivalent metal ions = −3 [16]. The valence of nitrogen is considered to be zero. Accordingly, the oxidizing and reducing valences of the compounds used in the combustion mixture can be calculated. In order to have the same oxidizing and reducing valences, the total ratio of the oxidizing to the reducing valences was one [17]. A 15 ml of solution containing nitrates and urea was added to a crucible. Then, the crucible containing the solution was introduced into a microwave oven. Initially, the solution boils and undergoes dehydration followed by decomposition with the evolution of large amounts of gases. After the solution reaches the point of spontaneous combustion, it begins burning and releases a lot of heat, instantly vaporizes the entire solution and becomes a solid, burning at a high temperature. The powder samples prepared by microwave-induced combustion process were pelletized and sintered at 1450 °C for 3 h. The bulk densities of the sintered samples were greater than 95% of the theoretical densities in all specimens.

2.2. Characterization measurements

A computer-interfaced X-ray powder diffractometer (XRD) with Cu Kα radiation (λ = 1.5418 Å) (Model Rigaku D/Max-II, Tokyo, Japan) was used to identify the crystalline phase and calculate crystallite size. The crystalline size, D_{XRD} was calculated according to Scherer's equation [18]: $D_{XRD} = 0.9\,\lambda / B\cos\theta$, where λ is the wavelength of the radiation, θ the diffraction angle, and B is the corrected half-width of the diffraction peak, give by $B^2 = B_m^2 - B_s^2$, where B_m is the measured half-width of the diffraction peak and B_s is the half-width of a standard CeO_2 with a crystal size greater than 100 nm. The reflection from (1 1 1) plane, occurring at 28.6° 2θ, was used to calculate the crystallite size. The morphological features of the particle were observed using a scanning electron microscope (SEM; Model JEOL JSM-6500F, Tokyo, Japan). For sintered specimens, the ionic conductivity was measured by the two-point DC method on a sintered $Ce_{0.8}(Gd_{0.2-x}Sm_x)O_{1.90}$ pellet. The two electrodes were formed by applying platinum paste to the two ends of the pellet and firing at 800 °C for 1 h. The ionic conductivity measurements were made at various temperatures in the range of 500–850 °C in air. Arrhenius plots (plots of $\ln\sigma$ vs. $10^3/T$) were constructed and activation energies for conduction were computed. The densities and porosities of the sintered ceramics were measured by the Archimedean method. The thermal expansion coefficients of sintered $Ce_{0.8}(Gd_{0.2-x}Sm_x)O_{1.90}$ pellets were measured by dilatometer (DIL; Model Netzsch DIL 402 PC, Bavaria, Germany) using a constant heating rate of 10 °C/min in the temperature range of 25–850 °C.

3. Results and discussion

The X-ray diffraction patterns of the $Ce_{0.8}(Gd_{0.2-x}Sm_x)O_{1.90}$ powders prepared by microwave-induced combustion process were identified by the diffractometer. Fig. 1 shows that the $Ce_{0.8}(Gd_{0.2-x}Sm_x)O_{1.90}$ powders contain only the cubic fluorite structure. The formation of single phase is due to the high temperature in situ generated during combustion and to the rapid cooling rate. Such high temperature could provide energy to produce doped cerium oxide powder from solution during combustion. It can be found that the XRD patterns peaks are

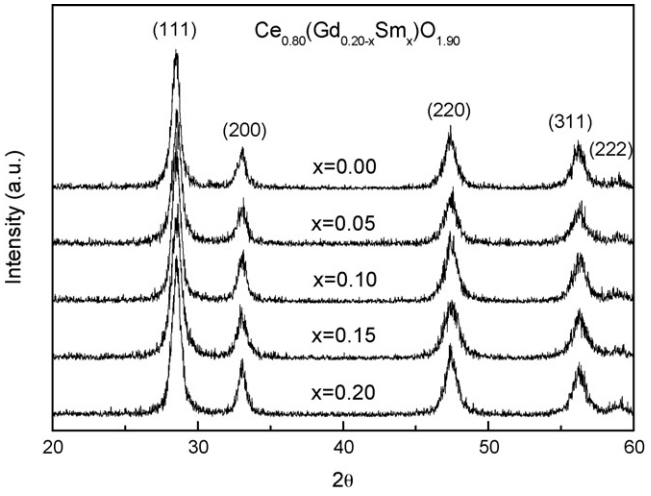

Fig. 1. XRD patterns of $Ce_{0.8}(Gd_{0.2-x}Sm_x)O_{1.90}$ powders prepared by microwave-induced combustion.

quite broad and indicate the fine particle of the product. The primary crystalline size determined from the Scherer's equation is about 10–20 nm in $Ce_{0.8}(Gd_{0.2-x}Sm_x)O_{1.90}$ samples. When using the Scherer's equation, we assume that the particle size effects are only from peak broadening; however, if the particles are non-uniform, the particle size will be underestimated. Fig. 2 represents scanning electron micrograph of $Ce_{0.80}Gd_{0.20}O_{1.90}$ specimens. It reveals that $Ce_{0.80}Gd_{0.20}O_{1.90}$ powders prepared by microwave-induced combustion have a nanostructure but are heavily agglomerated. Similar images are also found in the other Sm substitution powders. The particle size obtained by SEM does not depend on the substitution amount of samarium. The as-received $Ce_{0.80}Gd_{0.20}O_{1.90}$ powders showed a primary particle size from 20 to 30 nm. During the combustion synthesis, the powders had been exposed to a high temperature and necking between the particles seems to have had occurred.

Fig. 3 displays the XRD patterns of $Ce_{0.8}(Gd_{0.2-x}Sm_x)O_{1.90}$ ceramics, which powders derived from microwave-induced combustion process, with the fluorite structure in range of $x = 0.00$–0.20. No secondary phases are found in all specimens. It indicates a very large dopant concentration range sintered for $Ce_{0.8}(Gd_{0.2-x}Sm_x)O_{1.90}$ ceramics sintered at 1450 °C. The introduction of Sm_2O_3 into gadolinium-doped ceria (GDC) can cause a small shift in the GDC peaks. This shift is indicative of change in lattice parameter. A distribution of different Gd-doped concentrations within individual particles as well as between particles would lead to distribution of 2θ values. Fig. 4 shows the lattice constant of $Ce_{0.8}(Gd_{0.2-x}Sm_x)O_{1.90}$ ceramics as a function of Gd and Sm-doped concentration, x. Calculation of the cell parameters was carried out using the four main reflections typical of a fluorite structure material with a fcc cell, corresponding to the (1 1 1), (2 0 0), (2 2 0), and (3 1 1) plane. The lattice constant increased with Sm substitution amount for Gd in $Ce_{0.8}(Gd_{0.2-x}Sm_x)O_{1.90}$ ceramics. It indicates different radii of Gd^{3+} (0.97 Å) and Sm^{3+} (1.00 Å) in an oxide solid solution with a fluorite-type structure. Substitution Sm for Gd in GDC lattice will induce uniform strain in the lattice as the material is elastically deformed. This effect causes the lattice

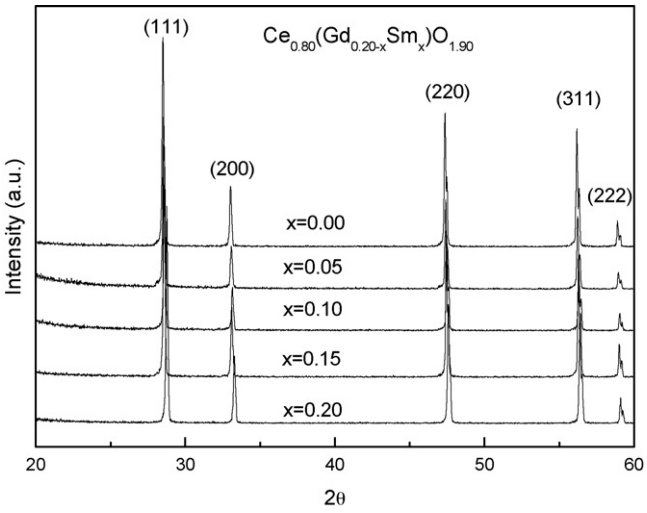

Fig. 3. XRD patterns of $Ce_{0.8}(Gd_{0.2-x}Sm_x)O_{1.90}$ ceramics sintered at 1450 °C for 3 h.

plane spacing to change and the diffraction peaks to shift to new 2θ position. As the Sm-substituted amount increase, the lattice constant increases linearly as $a(x) = 5.39754 + 0.134x$ for $Ce_{0.8}(Gd_{0.2-x}Sm_x)O_{1.90}$ ceramics ($x = 0.00$–0.20).

The ionic conductivity of $Ce_{0.8}(Gd_{0.2-x}Sm_x)O_{1.90}$ ceramics as a function of temperature and different Sm substitution are plotted in Figs. 5 and 6. It is found that $Ce_{0.80}Gd_{0.20}O_{1.90}$ specimen possessed the maximum ionic conductivity, 0.051 S/cm at 850 °C, the minimum activation energy, $E_a = 0.77$ eV in the temperature range of 500–850 °C and minimum thermal expansion coefficient, TEC = 18.733 ppm/°C in the temperature range of 25–850 °C. Similar ionic conductivity results have been found in previous literatures [19]. This result indicated that $Ce_{0.80}Gd_{0.20}O_{1.90}$ ceramic derived from microwave-induced combustion process possessed good ionic conductivity. With temperature increasing, the oxygen ion mobility increases, and consequently the conductivities increase. It is found that the conductivity for $Ce_{0.8}Sm_{0.2}O_{1.9}$ ($x = 0.20$) have the highest value at low temperature range (500–650 °C) but it

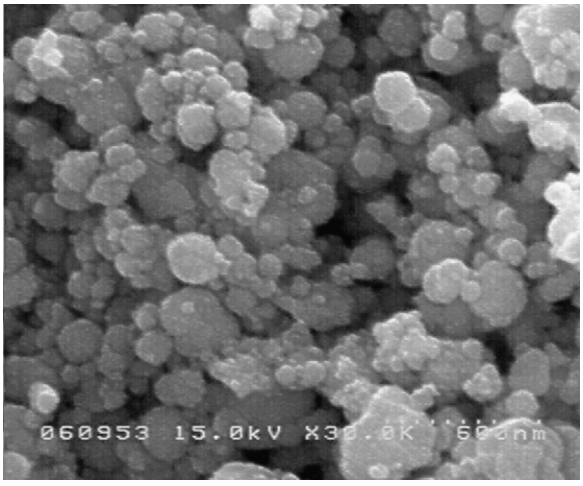

Fig. 2. Scanning electron micrograph of $Ce_{0.80}Gd_{0.20}O_{1.90}$ powder prepared by microwave-induced combustion.

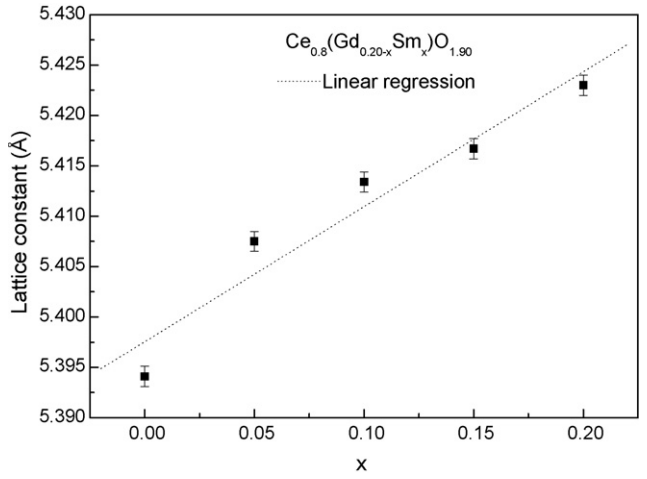

Fig. 4. Lattice constant of $Ce_{0.8}(Gd_{0.2-x}Sm_x)O_{1.90}$ ceramics as function of Sm-substituted amount.

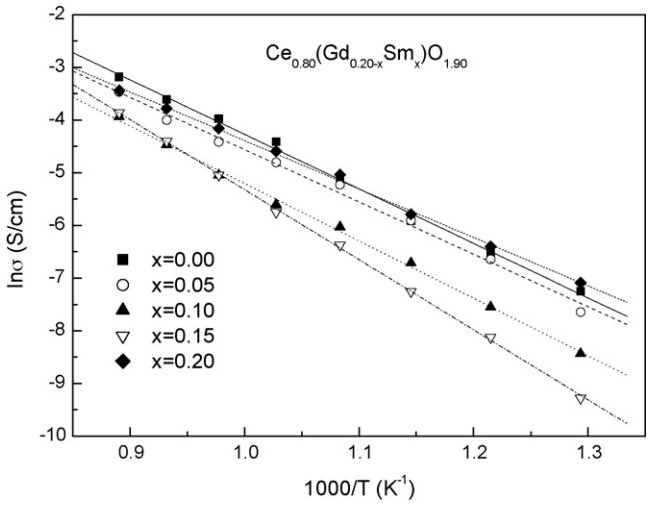

Fig. 5. Arrhenius plots for ionic conductivities of $Ce_{0.8}(Gd_{0.2-x}Sm_x)O_{1.90}$ ceramics.

becomes less than $Ce_{0.8}Gd_{0.2}O_{1.9}$ ($x = 0.00$) at high temperature range (650–850 °C). It indicates that $Ce_{0.80}Sm_{0.20}O_{1.90}$ possessed higher ionic conductivity than $Ce_{0.80}Gd_{0.20}O_{1.90}$ below 650 °C, whereas, $Ce_{0.80}Gd_{0.20}O_{1.90}$ with highest ionic conductivity is found above 650 °C. Activation energy for conduction is obtained by plotting the ionic conductivity data in Arrhenius relation for thermally activated conduction. Activation energy was calculated according to following equation. $\sigma T = \sigma_0 \exp(-E_a/kT)$, where E_a is the activation energy for conduction, T the absolute temperature, and σ_0 is a pre-exponential factor [20]. Activation energy for $Ce_{0.8}(Gd_{0.2-x}Sm_x)O_{1.90}$ ceramics are summarised in Table 1. Fig. 7 displays the variation of the activation energy, E_a as a function of Sm-substituted amount in $Ce_{0.8}(Gd_{0.2-x}Sm_x)O_{1.90}$ ceramics in the temperature range of 500–850 °C. The activation energy increases gradually with increasing Sm-substituted amount and reaches a maximum, $E_a = 1.15$ eV for $Ce_{0.80}(Gd_{0.05}Sm_{0.15})O_{1.92}$ specimen. Further increasing the Sm-substituted amount for $x > 0.15$ leads to a fall in activation

Table 1
The average linear thermal expansion coefficients, and activation energy, for $Ce_{0.8}(Gd_{0.2-x}Sm_x)O_{1.90}$ ceramics

Nominal composition	Linear thermal expansion ($\times 10^{-6}$)	Activation energy, E_a (eV)
$Ce_{0.8}Gd_{0.2}O_{1.9}$	18.7336	0.7718
$Ce_{0.8}(Gd_{0.15}Sm_{0.05})O_{1.9}$	19.3042	0.9373
$Ce_{0.8}(Gd_{0.10}Sm_{0.10})O_{1.9}$	19.5699	1.1435
$Ce_{0.8}(Gd_{0.05}Sm_{0.15})O_{1.9}$	19.8311	1.1507
$Ce_{0.8}Sm_{0.2}O_{1.9}$	19.1391	0.8541

energy. The $Ce_{0.8}(Gd_{0.2-x}Sm_x)O_{1.90}$ powders synthesized by microwave-induced combustion process can significantly decrease the sintering temperature of $Ce_{0.8}(Gd_{0.2-x}Sm_x)O_{1.90}$ ceramics, compared to that above 1550 °C required for ceria solid electrolytes prepared by solid state reaction. Apart from high ion conductivity, the electrolyte materials for SOFC must have matched thermal expansion coefficient for cathode and anode materials to avoid microcrack between anode and electrolyte or between cathode and electrolyte at operation temperature. The average thermal expansion coefficient of $Ce_{0.8}(Gd_{0.2-x}Sm_x)O_{1.90}$ ceramics versus Sm-substituted amount is depicted in Fig. 8. It reveals that the thermal expansion coefficient of $Ce_{0.8}(Gd_{0.2-x}Sm_x)O_{1.90}$ ceramics initially increases with increasing Sm-substituted amount in range of $x = 0.00$–0.15. A minimum thermal expansion coefficient is 18.733 ppm/°C for $Ce_{0.80}Gd_{0.20}O_{1.90}$ specimen. Further increasing the Sm-substituted amount leads to an increase in thermal expansion coefficient and reaches a maximum, TEC = 19.831 ppm/°C for $Ce_{0.80}(Gd_{0.05}Sm_{0.15})O_{1.92}$ specimen. A bulk thermal expansion study on $Ce_{0.8}(Gd_{0.2-x}Sm_x)O_{1.90}$ ceramics has been conducted from room temperature to 800 °C using a dilatometer. In order to investigate the bulk thermal expansion behavior versus temperature for $Ce_{0.8}(Gd_{0.2-x}Sm_x)O_{1.90}$ system. A typical plot of linear thermal expansion (in percent) as function of temperature is shown in Fig. 9. It revealed that linear thermal

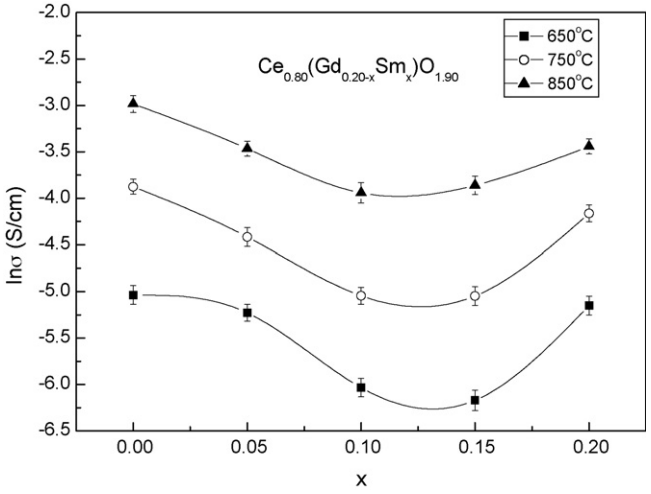

Fig. 6. Sm-substituted amount dependence of ionic conductivities of $Ce_{0.8}(Gd_{0.2-x}Sm_x)O_{1.90}$ ceramics at different temperatures.

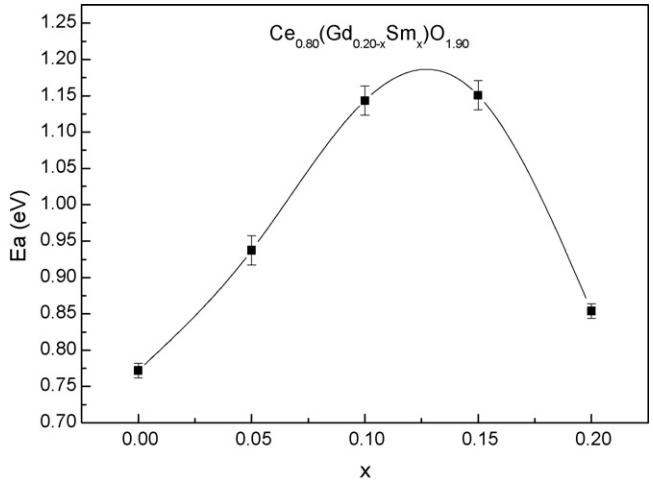

Fig. 7. Variation of activation energy, E_a as function of Sm-substituted amount in $Ce_{0.8}(Gd_{0.2-x}Sm_x)O_{1.90}$ ceramics in temperature range of 500–850 °C.

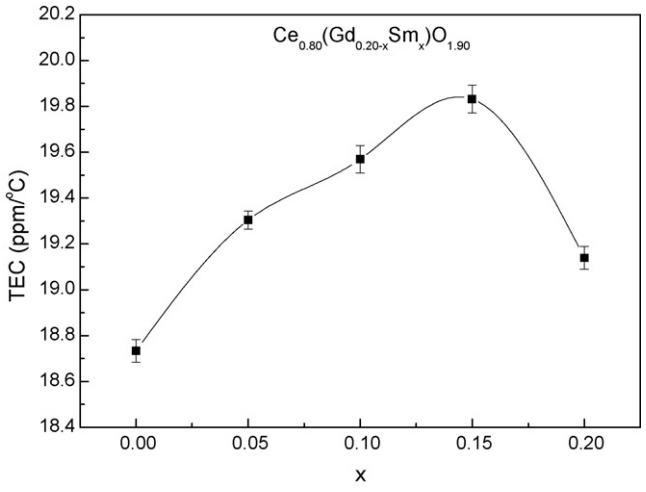

Fig. 8. The thermal expansion coefficient of $Ce_{0.8}(Gd_{0.2-x}Sm_x)O_{1.90}$ ceramics vs. Sm-substituted content.

expansion fitted as a function of temperature using a polynomial regression. The polynomial correlations are given as follows (temperature, T, in centigrade):

- For $Ce_{0.8}(Gd_{0.1}Sm_{0.1})O_{1.9}$:

$$100\frac{\Delta L}{L_0} = -0.03239 + (8.50966 \times 10^{-4})T + (2.5423 \times 10^{-6})T^2 - (2.83766 \times 10^{-9})T^3 + (1.51966 \times 10^{-12})T^4$$

- For $Ce_{0.8}(Gd_{0.05}Sm_{0.15})O_{1.9}$:

$$100\frac{\Delta L}{L_0} = -0.03347 + (8.14722 \times 10^{-4})T + (2.75562 \times 10^{-6})T^2(2.69781 \times 10^{-9})T^3 + (1.35002 \times 10^{-12})T^4$$

- For $Ce_{0.8}(Gd_{0.15}Sm_{0.05})O_{1.9}$:

$$100\frac{\Delta L}{L_0} = -0.05859 + (0.00156)T - (1.5709 \times 10^{-6})T^2 + (5.2394 \times 10^{-9})T^3 - (3.355941 \times 10^{-12})T^4$$

- For $Ce_{0.8}Sm_{0.2}O_{1.9}$:

$$100\frac{\Delta L}{L_0} = 0.03376 + (8.98333 \times 10^{-4})T + (2.0328 \times 10^{-6})T^2 - (1.8016 \times 10^{-9})T^3 + (8.7337 \times 10^{-13})T^4$$

- For $Ce_{0.8}Gd_{0.2}O_{1.9}$:

$$100\frac{\Delta L}{L_0} = -0.02963 + (8.07853 \times 10^{-4})T + (2.6418 \times 10^{-6})T^2 - (2.71294 \times 10^{-9})T^3 + (1.3796 \times 10^{-12})T^4$$

The average linear thermal expansion coefficients in the temperature range of 25–850 °C for $Ce_{0.8}(Gd_{0.2-x}Sm_x)O_{1.90}$ ceramics are shown in Table 1.

The correlation between thermal expansion coefficient and the logarithm of the ionic conductivity for $Ce_{0.8}(Gd_{0.2-x}Sm_x)O_{1.90}$ ceramics is shown in Fig. 10. It indicates that Sm-substituted GDC ceramics with higher conductivity but possessed lower thermal expansion coefficient. According to this viewpoint, we can easily predict the ionic conductivity property of Sm-substituted GDC ceramics by the measurement of thermal expansion coefficient. The thermal expansion coefficient in the range of 25–850 °C and ion conductivity at 650 °C for $Ce_{0.8}(Gd_{0.2-x}Sm_x)O_{1.90}$ ceramics give the polynomial correlation as follows:

$$\mathrm{TEC} = -1940.77 - 1277.25(\ln\sigma) - 309.15(\ln\sigma)^2 - 32.83(\ln\sigma)^3 - 1.29(\ln\sigma)^4$$

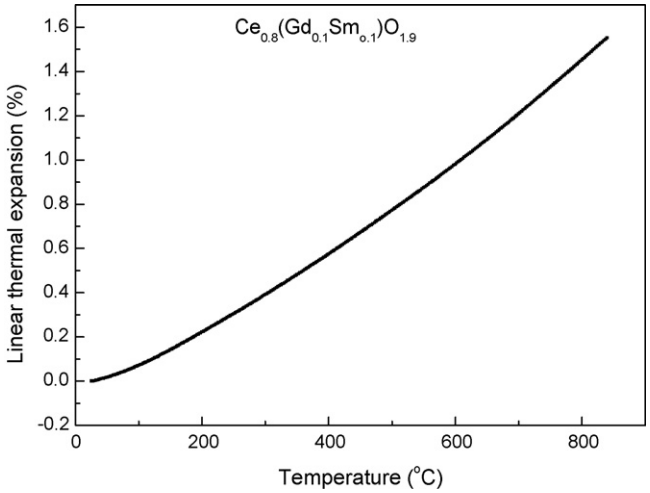

Fig. 9. Linear thermal expansion of $Ce_{0.8}(Gd_{0.1}Sm_{0.1})O_{1.9}$ ceramic as function of temperature in the temperature range of 25–850 °C.

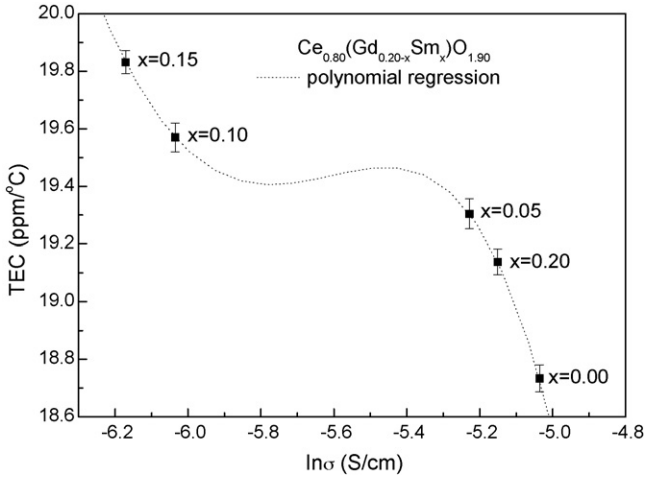

Fig. 10. Correlation between thermal expansion coefficient, TEC (25–850 °C) and ionic conductivity,σ (650 °C, air) for $Ce_{0.8}(Gd_{0.2-x}Sm_x)O_{1.90}$ ceramics.

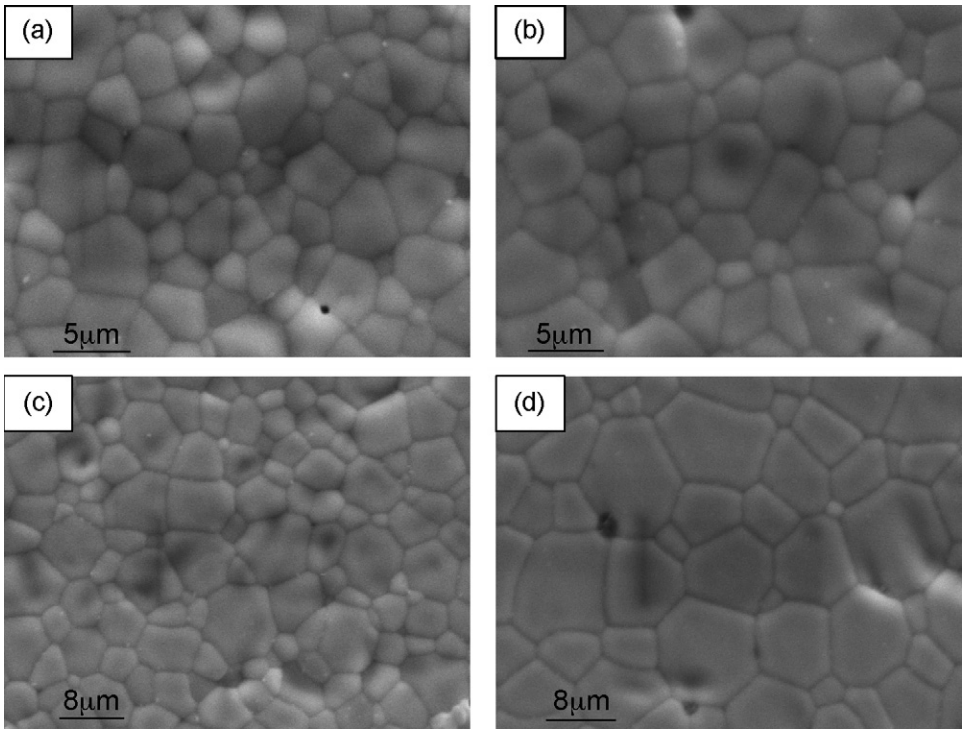

Fig. 11. SEM micrographs of sintered $Ce_{0.8}(Gd_{0.2-x}Sm_x)O_{1.90}$ ceramics of (a) $Ce_{0.8}Gd_{0.2}O_{1.9}$, (b) $Ce_{0.8}(Gd_{0.15}Sm_{0.05})O_{1.9}$, (c) $Ce_{0.8}(Gd_{0.10}Sm_{0.10})O_{1.9}$, and (d) $Ce_{0.8}(Gd_{0.05}Sm_{0.15})O_{1.9}$.

The correlation obtained provides an empirical evaluation of the properties of $Ce_{0.8}(Gd_{0.2-x}Sm_x)O_{1.90}$ ceramics if the other one is known. Fig. 11 shows the morphology of $Ce_{0.8}(Gd_{0.2-x}Sm_x)O_{1.90}$ ceramics. The microstructure of $Ce_{0.8}(Gd_{0.2-x}Sm_x)O_{1.90}$ ceramics revealed that high densification was achieved. There was little or no intergranular porosity can be found in all specimens. In Fig. 11(a), it revealed that the average grain size of $Ce_{0.8}Gd_{0.2}O_{1.9}$ was about 1–2 μm, which is associated with the superfine primary powder. These microstructure characteristic may be in favor of improving the grain interior conductivity [21]. The theory density of all specimens was greater than 95%. Moreover, it is found that the grain size increases with the amount of Sm substitution for Gd in $Ce_{0.8}(Gd_{0.2-x}Sm_x)O_{1.90}$ system for $0.00 \leq x \leq 0.15$. In Fig. 11(d), the grain boundaries tend to merge and the grains size become larger. The grain is distributed over the range of 3–5 μm. With regard to the grain size increases for $x = 0.15$ in $Ce_{0.8}(Gd_{0.2-x}Sm_x)O_{1.90}$ system, the mechanism does not realize clearly at present stage. This behavior is related with the thermal expansion and activation energy results. It implied that the amount of Sm has a strong effect on microstructure and grain size in $Ce_{0.8}(Gd_{0.2-x}Sm_x)O_{1.90}$ system for $0.00 \leq x \leq 0.15$. According to the thermal expansion, activation, and SEM results, it concluded that the specimen with large grain size possessed higher thermal expansion coefficient and activation energy for $Ce_{0.8}(Gd_{0.2-x}Sm_x)O_{1.90}$ ($0.00 \leq x \leq 0.15$.) system.

4. Conclusions

In this study, using cerium nitrate hexahydrate, gadolinium nitrate hexahydrate, samarium nitrate hexahydrate, and urea as the starting materials, $Ce_{0.8}(Gd_{0.2-x}Sm_x)O_{1.90}$ nanopowders have been synthesized successfully by microwave-induced combustion process. $Ce_{0.8}(Gd_{0.2-x}Sm_x)O_{1.90}$ ceramics were sintered at 1450 °C for 3 h, the bulk density was over 95% of the theoretical density. The maximum ionic conductivity, $\sigma_{850^\circ C} = 0.051$ S/cm, minimum activation energy, $E_a = 0.77$ eV and minimum thermal expansion coefficient, TEC = 18.733 ppm/°C was found at $Ce_{0.80}Gd_{0.20}O_{1.90}$ ceramic. It seems to have some correlation between the thermal expansion, grain size, and activation energy. According to experimental results, it is concluded that the specimen with large grain size possessed higher thermal expansion coefficient and activation energy in $Ce_{0.8}(Gd_{0.2-x}Sm_x)O_{1.90}$ for $0.00 \leq x \leq 0.15$.

Acknowledgement

The author would like to thank the National Science Council of the Republic of China for financially supporting this research under Contract no. NSC 94-2216-E-259-008.

References

[1] N.Q. Minh, Ceramic fuel cells, J. Am. Ceram. Soc. 76 (3) (1993) 563–588.
[2] H.L. Tuller, Ionic conduction in nanocrystalline materials, Solid State Ionics 131 (2000) 143–157.
[3] S. Dikmen, P. Shuk, M. Greenblatt, H. Gocmez, Hydrothermal synthesis and properties of $Ce_{1-x}Gd_xO_{2-\delta}$ solid solutions, Solid State Sci. 4 (2002) 585–590.
[4] S. Zha, C. Xia, G. Meng, Effect of Gd (Sm) doping on properties of ceria electrolyte for solid oxide fuel cells, J. Power Sources 115 (2003) 44–48.

[5] Y. Gu, G. Li, G. Meng, D. Peng, Sintering and electrical properties of coprecipitation prepared $Ce_{0.8}Y_{0.2}O_{1.9}$ ceramics, Mater. Res. Bull. 35 (2) (2000) 297–304.
[6] T.S. Zhang, J. Ma, L.B. Kong, P. Hing, J.A. Kliner, Preparation and mechanical properties of dense $Ce_{0.8}Gd_{0.2}O_{2-\delta}$ ceramics, Solid State Ionics 167 (2004) 191–196.
[7] A. Sin, Y. Dubitsky, A. Zaopo, A.S. Airco, L. Gullo, D.L. Rosa, S. Siracusao, V. Antonucci, C. Oliva, O. Ballabio, Preparation and sintering of $Ce_{1-x}Gd_xO_{2-x/2}$ nanopowders and their electrochemical and EPR characterization, Solid State Ionics 175 (2004) 361–366.
[8] N. Kim, B.-H. Kim, D. Lee, Effect of co-dopant addition on properties of gadolinia-doped ceria electrolyte, J. Power Sources 90 (2000) 139–143.
[9] R.D. Purohit, B.P. Sharma, K.T. Pillai, A.K. Tyagi, Ultrafine ceria powder via glycine–nitrate combustion, Mater. Res. Bull. 36 (2001) 2711–2721.
[10] R. Peng, C. Xia, Q. Fu, G. Meng, D. Peng, Sintering and electrical properties of $(CeO_2)_{0.8}(Sm_2O_3)_{0.1}$ powders prepared by glycine–nitrate process, Mater. Lett. 56 (2002) 1043–1047.
[11] J.J. Kingsley, K. Suresh, K.C. Patil, Combustion synthesis of fine-particle metal aluminates, J. Mater. Sci. Lett. 29 (1990) 1305–1312.
[12] D.E. Clark, W.H. Sutton, Microwave processing of materials, Ann. Rev. Mater. Sci. 26 (1996) 299–331.
[13] O.A. Lopez, J. McKittrick, L.E. Shea, Fluorescence properties of polycrystalline Tm^{+++}-activated $Y_3Al_5O_{12}$ and Tm^{+++}–Li^+ co-activated $Y_3Al_5O_{12}$ in the visible and near IR ranges, J. Lumin. 71 (1997) 1–11.
[14] S.V. Chavan, M.D. Mathew, A.K. Tyagi, Phase relation and thermal expansion studies in ceria-yttria system, J. Am. Ceram. Soc. 87 (2004) 1977–1980.
[15] S.R. Jain, K.C. Adiga, V.R.P. Verneker, A new approach to thermochemical calculations of condensed fuel-oxidizer mixtures, Combust. Flame 40 (1981) 71–79.
[16] R. Gopi Chandran, K.C. Patil, G.T. Chandrappa, Combustion synthesis, characterization, sintering and microstrucutre of mullite–cordierite composites, J. Mater. Sci. Lett. 14 (1995) 548–551.
[17] H.K. Park, Y.S. Han, D.K. Kim, C.H. Kim, Synthesis of $LaCrO_3$ powders by microwave-induced combustion of metal nitrate–urea mixture solution, J. Mater. Sci. Lett. 17 (1998) 785–787.
[18] H.P. Klug, L.E. Alexander, X-ray Diffraction Procedures, Wily, New York, 1974.
[19] J. Ma, T.S. Zhang, L.B. Kong, P. Hing, S.H. Chan, $Ce_{0.8}Gd_{0.2}O_{2-\delta}$ ceramics derived from commercial submicron-sized CeO_2 and Gd_2O_3 powders for use as electrolytes in solid oxide fuel cells, J. Power Sources 132 (2004) 71–76.
[20] C. Tian, S.-W. Chan, Ionic conductivities, sintering temperatures and microstructures of bulk ceramic CeO_2 doped with Y_2O_3, Solid State Ionics 134 (2000) 89–102.
[21] X.T. Su, Q.Z. Yan, X.H. Ma, W.F. Zhang, C.C. Ge, Effect of co-dopant addition on the properties of yttrium and neodymium doped barium cerate electrolyte, Solid State Ionics 177 (2006) 1041–1045.